Cerebral Cortex April 2015;25:918–926
doi:10.1093/cercor/bht280
Advance Access publication October 9, 2013

Visual Cortical Gamma-Band Activity During Free Viewing of Natural Images

Nicolas Brunet[1,2], Conrado A. Bosman[1,3], Mark Roberts[1,4], Robert Oostenveld[1], Thilo Womelsdorf[1], Peter De Weerd[1,4] and Pascal Fries[1,5]

[1]Donders Institute for Brain, Cognition, and Behaviour, Radboud University Nijmegen, 6525 EN Nijmegen, The Netherlands, [2]Department of Neurological Surgery, University of Pittsburgh, PA 15213, USA, [3]Cognitive and Systems Neuroscience Group, Swammerdam Institute for Life Sciences, Center for Neuroscience, University of Amsterdam, 1098 XH Amsterdam, The Netherlands, [4]Department of Neurocognition, University of Maastricht, 6229 ER Maastricht, The Netherlands and [5]Ernst Strüngmann Institute (ESI) for Neuroscience in Cooperation with Max Planck Society, 60528 Frankfurt, Germany

Address correspondence to Pascal Fries, Ernst Strüngmann Institute (ESI) for Neuroscience in Cooperation with Max Planck Society, Deutschordenstr. 46, 60528 Frankfurt, Germany. Email: pascal.fries@esi-frankfurt.de

N.B. and C.A.B. contributed equally to this work.

Gamma-band activity in visual cortex has been implicated in several cognitive operations, like perceptual grouping and attentional selection. So far, it has been studied primarily under well-controlled visual fixation conditions and using well-controlled stimuli, like isolated bars or patches of grating. If gamma-band activity is to subserve its purported functions outside of the laboratory, it should be present during natural viewing conditions. We recorded neuronal activity with a 252-channel electrocorticographic (ECoG) grid covering large parts of the left hemisphere of 2 macaque monkeys, while they freely viewed natural images. We found that natural viewing led to pronounced gamma-band activity in the visual cortex. In area V1, gamma-band activity during natural viewing showed a clear spectral peak indicative of oscillatory activity between 50 and 80 Hz and was highly significant for each of 65 natural images. Across the ECoG grid, gamma-band activity during natural viewing was present over most of the recorded visual cortex and absent over most remaining cortex. After saccades, the gamma peak frequency slid down to 30–40 Hz at around 80 ms postsaccade, after which the sustained 50- to 80-Hz gamma-band activity resumed. We propose that gamma-band activity plays an important role during natural viewing.

Keywords: ECoG, free viewing, gamma, natural image, oscillation

Introduction

Neuronal gamma-band synchronization in visual cortex has been associated with several important functions, particularly perceptual grouping and selection (Eckhorn et al. 1988; Gray et al. 1989; Kreiter and Singer 1996; Livingstone 1996; Fries et al. 1997; Gail et al. 2000), attentional stimulus selection (Fries, Reynolds, et al. 2001; Bichot et al. 2005; Taylor et al. 2005; Bauer et al. 2006; Womelsdorf et al. 2006; Fries et al. 2008; Buffalo et al. 2011; Bosman et al. 2012; Grothe et al. 2012), and efficient stimulus representation and signaling (Womelsdorf et al. 2007; Hoogenboom et al. 2010; Vinck et al. 2010; Womelsdorf et al. 2012; Roberts et al. 2013). All of these studies used artificial stimuli, like bars, gratings, letter-like symbols, or Bezier curves, always on uniform backgrounds.

If gamma-band synchronization plays a role in stimulus processing, perceptual grouping, or selective attention during natural viewing, it needs to be present during free viewing of natural images. So far, this has not been demonstrated, but to the contrary, several studies strongly suggest that free viewing of natural images eliminates gamma-band activity. A previous study used an interesting approach when aiming to emulate natural viewing (Kayser et al. 2003). The authors first mounted a camera onto the head of a cat and recorded movies while the cat roamed through nature. Subsequently, they presented these movies to an awake head-fixed cat and recorded neuronal activity from primary visual cortex. They report that such movies primarily induce broad-band local field potential (LFP) power increases between 100 and 200 Hz, which differ strongly from band-limited gamma (40–80 Hz) power increases that they find for grating stimuli, and rather resemble power changes that they observe when presenting pink-noise stimuli. Another recent study investigated single units and LFP in area V1 of cebus monkeys freely viewing natural images (Ito et al. 2011). These authors focus on saccade-related modulations of coincident spiking and of LFP locking. Yet, as an example, they also show a time–frequency analysis of LFP power (their Fig. 1*C*) and, while it reveals alpha- and beta-band modulations, there are no clear gamma-band peaks.

Other studies demonstrated that gamma-band activity is strongly reduced for grating stimuli of reduced size (Gieselmann and Thiele 2008) or for 2 gratings superimposed to form a plaid (Lima et al. 2010). Natural images often contain small and/or superimposed components and might, therefore, induce only marginal gamma-band activity. Finally, the frequency of gamma-band activity can shift by at least 25 Hz upon changes in stimulus properties like size (Gieselmann and Thiele 2008) or contrast (Ray and Maunsell 2010; Roberts et al. 2013). Therefore, natural images with their wide range of object sizes and contrasts might lead to local gamma-band activities with a wide range of frequencies, which might not summate effectively and thereby lead to merely weak and broad-band power increases.

Since an absence of gamma-band activity during free viewing of natural images would seriously question its hypothesized functions, we reinvestigated this issue. We recorded LFP from electrocorticographic (ECoG) grid electrodes covering areas V1, V4, and several additional areas of the left hemisphere in 2 macaque monkeys freely viewing natural images.

Materials and Methods

Stimuli and Behavioral Paradigm

All animal procedures were approved by the ethics committee of the Radboud University, Nijmegen, Netherlands. Two adult male macaque monkeys were used in this study and we will refer to them as monkey

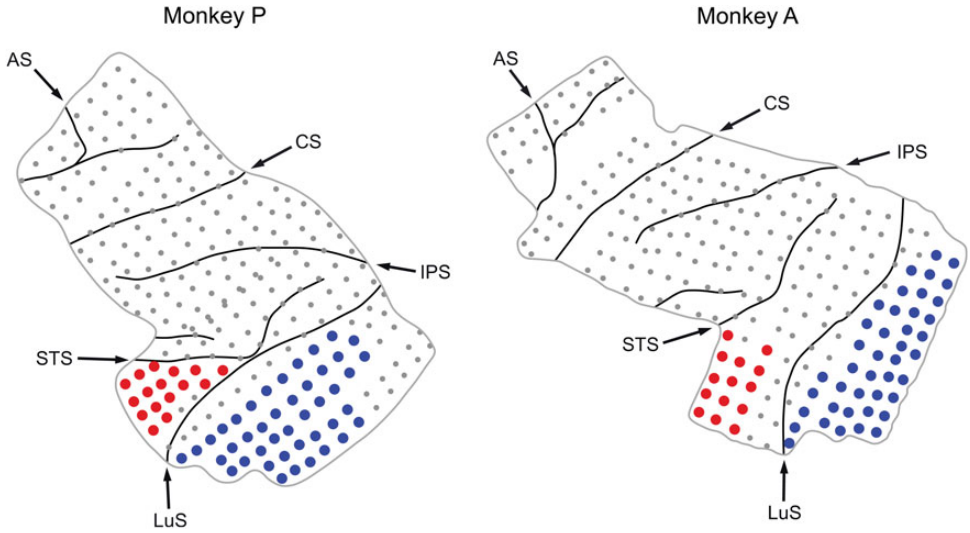

Figure 1. Positions of electrodes and sulci and definition of V1 and V4 electrodes. The 2 panels are rendered from photographs taken during the electrode implantation surgeries, after placement of the ECoG grid onto the brain, before closure of the dura. The outer border corresponds to the total area covered by the ECoG grid. The lines inside the border correspond to the major sulci. LuS: lunate sulcus; STS: superior temporal sulcus; AS: arcuate sulcus; CS: central sulcus; IPS: intraparietal sulcus. Small black dots indicate the positions of all 252 electrodes. Large blue (red) dots indicate the positions of electrodes assigned to area V1 (V4).

P and monkey A. Monkey P in this study is the same as monkey P in Bosman et al. (2012). We presented stimuli and controlled behavior with the CORTEX system. Stimuli were presented on a cathode ray tube (CRT) screen refreshing at 120 Hz noninterlaced and positioned such that 32 pixels corresponded to 1° of visual angle (°).

The monkeys were trained to perform different tasks, while having their head fixed. For the data reported in this study, monkeys were required to fixate for 0.63 s on a fixation point (0.12 by 0.12° black square) centered on a gray background, after which a natural image was presented, which was again centered on the background screen. Grayscale images were shown for 3.5–6 s (flat random distribution), and color images for 1.5 s. Once the image had appeared on the screen, the monkey could view it freely. If the monkey kept its gaze on the image as long as it was presented, it was given a juice reward after stimulus offset. Because this task was very easy for the monkeys, almost every trial was rewarded. We used 49 grayscale images and 16 color images, with grayscale and color images presented in separate sessions. Grayscale images subtended 16-by-16°, and color images 18.5-by-18.5°. Each grayscale image was presented for an average of 15 trials, and each color image for an average of 22 trials. Eye position was recorded with an infrared camera system (Thomas Recording ET-49B system) at a sampling rate of 230 Hz.

Data Acquisition

The monkeys were implanted with ECoG grid electrodes, consisting of 252 subdural electrodes distributed across several superficial areas (Rubehn et al. 2009; Bosman et al. 2012). Unless stated otherwise, we selected electrodes over V1 and V4 that were strongly driven by stimuli within the central 4° of eccentricity. Due to placement of the ECoG grid onto the dorsal parts of V1 and V4 in the left hemisphere, receptive fields were in the lower right visual quadrant. Correspondingly, we accepted analysis epochs when the gaze of the monkey was at least 4° away from the lower and the right border of the natural image for at least 90% of the epoch duration. This ensured that the responses of the recorded sites were due to the natural image rather than the screen background. In monkey P (monkey A), we used 43 (42) electrodes on V1 and 16 (14) on V4. Those electrodes are highlighted as large, colored dots in Figure 1. The assignment of electrodes to visual areas was based on intraoperative photographs and brain atlases, and used primarily sulcal landmarks. For most of the electrodes, the area assignment was unequivocal. Yet, some of the most anterior electrodes assigned to V1 might as well be over V2, and the most lateral electrodes assigned to V4 might as well be over the temporal-occipital area (TEO). Exclusion of those electrodes left the results qualitatively unchanged.

Electrophysiological signals were impedance buffered and amplified 20 times through eight 32-channel headstages (Plexon Headstage 32 V-G20). They were then low-pass filtered at 8 kHz and digitized at roughly 32 kHz (Neuralynx Digital Lynx 256 channel system). Monkey P was recorded also while performing a selective visual attention task. Results from those recordings have been published along with more information on the typical receptive fields obtained with the ECoG electrodes (Bosman et al. 2012).

Data Analysis and Statistical Testing

All analyses were done in Matlab (The MathWorks), and using the FieldTrip open source Matlab toolbox (http://fieldtrip.fcdonders.nl/) (Oostenveld et al. 2011). Signals were low-pass filtered at 250 Hz and downsampled to 1 kHz. During recordings, the signal from each electrode was differentiated against a common reference and we refer to this signal as the unipolar LFP. Offline, signals from pairs of immediately neighboring electrodes were subtracted from each other to remove the common recording reference, and we refer to this bipolar derivation as a "site" and to the resulting signal as a bipolar or locally differentiated LFP or just as LFP. Power-line artifacts were removed by subtracting the discrete Fourier transforms at 50 and 100 Hz.

We performed frequency-resolved, that is, spectral, analyses of LFP power. For Figures 2–4, we limited data selection and processing to the absolute minimum. In Figure 2*B*, the analysis covered 20–140 Hz in steps of 2 Hz, using for each frequency an epoch length of 4 cycles. The resulting epochs were Hanning tapered and Fourier transformed. Figure 2*C* is based on 3 slightly overlapping 0.5 s epochs, multitapered with 8 tapers (Mitra and Pesaran 1999) to achieve an ±8-Hz spectral smoothing. Figures 3 and 4 are based on all nonoverlapping 0.5 s epochs from 0.3 s after stimulus onset until stimulus offset, during which the receptive fields (RFs) remained on the image (see above for details), compared with a 0.5-s prestimulus baseline. These epochs were Hanning tapered and Fourier transformed. For Figure 5, we aimed at focusing on the effect of visual processing during free viewing, rather than the effects of saccades. Therefore, we selected all 0.25 s epochs that started 0.125 s after a saccade and did not include the following saccade. Those epochs were Hanning tapered. Saccades were defined as follows: The vertical and horizontal eye position traces were low-pass filtered at 50 Hz, differentiated to obtain vertical and horizontal eye velocity, and combined to obtain overall eye speed. Eye speeds of >40°/s were considered saccades. The time of the saccade was defined as the moment of peak saccade velocity. Saccades following other saccades within <20 ms were discarded. In Figure 6, we investigated the dynamics of spectral power around the time of a

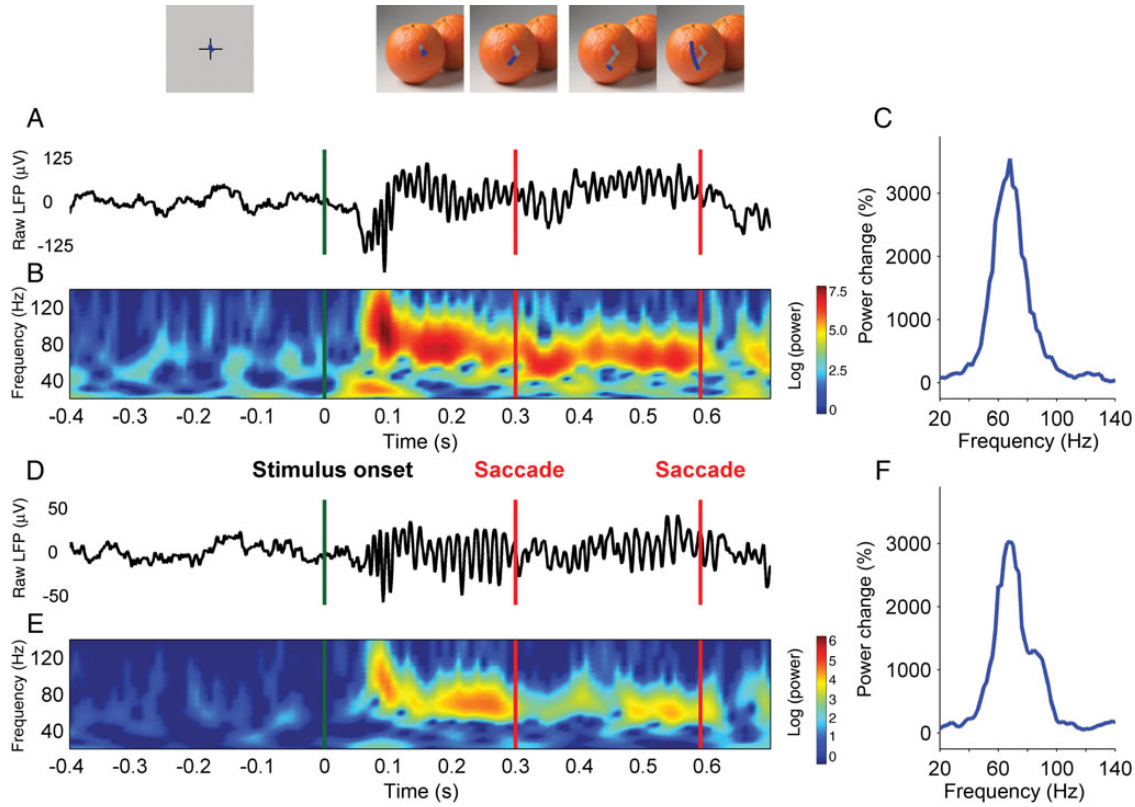

Figure 2. Gamma-band oscillation in the raw LFP of one example site during one example visual exploration. (*A*) Raw unipolar LFP trace during one visual exploration of the photograph of 2 oranges. The insets above the LFP show the stimulus presented to the monkey at the respective time point, and superimposed the eye position trace around that time point in blue, and the eye position trace during this exploration so far in gray. The fixation point is shown as a cross to make it visible behind the eye trace, while it was actually a small green square. (*B*) Time–frequency analysis of absolute power of the same example unipolar LFP. (*C*) Power change spectrum of the same unipolar LFP during visual exploration versus prestimulus baseline. (*D–F*) Same as (*A–C*) for an example locally bipolar LFP.

saccade. For this analysis, we selected epochs from 0.2 s before saccades until 0.3 s after the saccade, during which the RFs were on the image (see above for details). The subsequent time–frequency analysis was the same as in Figure 2*E*, that is, using 4 cycles per frequency, Hanning tapered. For Figure 6, we selected those V1 and V4 sites that showed the top third (V1) and top half (V4) gamma-band power increases during natural viewing. The gamma-frequency band was defined as 50–80 Hz in both monkeys. Where power during free viewing of natural images was normalized by power during the prestimulus baseline, the respective power values were first averaged across trials, separately for the 2 epochs, before normalization.

Results

Figure 2*A* shows an example raw, unipolar LFP trace of one electrode in area V1 recorded while monkey P explored a photograph of 2 oranges. The stimulus replaced the fixation point at time zero and, within <100 ms, the LFP was dominated by strongly rhythmic gamma-band oscillations. These LFP data were only filtered broadly, between 1 and 250 Hz. The time–frequency analysis of absolute power (Fig. 2*B*) shows that the gamma-band activity was band-limited with a peak between 50 and 80 Hz and largely sustained, with interruptions after saccades, as will be investigated in more detail later. Gamma-band activity was much weaker though not absent before stimulus onset. Figure 2*C* shows the change in spectral power during natural viewing when compared with the baseline, documenting a prominent gamma-band peak. Figure 2*D–F* shows the same example trial for a locally differentiated (i.e., bipolar) LFP, demonstrating that the gamma-band response in this signal was very similar to the unipolar LFP.

Among all images, the oranges induced the strongest gamma-band oscillations. Yet, clear gamma-band peaks could be seen in the power change spectra for all of the images and across most of the sites in V1 and V4. To document that gamma-band activity during free viewing of natural images was robust, we show 1) spectra averaged over V1 sites, separately for 24 example images (Fig. 3), 2) distributions of gamma power changes averaged over V1 sites and, corresponding *P*-values, separately for all images (Fig. 4), 3) spectra averaged over all images, separately for example V1, V4, and nonvisual sites (Fig. 5), 4) topographies of gamma power changes (and corresponding *t*-values) averaged over all images, characterizing gamma activity for each site across the ECoG grid (Fig. 5).

Figure 3 shows the power change spectra averaged over all sites in area V1, separately for the 2 monkeys (monkey P: red and monkey A: blue), for 12 grayscale and 12 color images. All power change spectra show a clear gamma-band peak. Figure 4 documents the corresponding peak gamma power changes across all natural images and demonstrates that each image individually induced a highly significant gamma power enhancement. Also, for each image, power enhancements during natural viewing compared with prestimulus baseline (i.e., log10 [power during natural viewing/power during prestimulus baseline]) were significantly stronger in the gamma-frequency band (50–80 Hz) when compared with a 150- to 200-Hz band (largest *P*-value was 0.0007, paired *t*-test across trials), indicating that

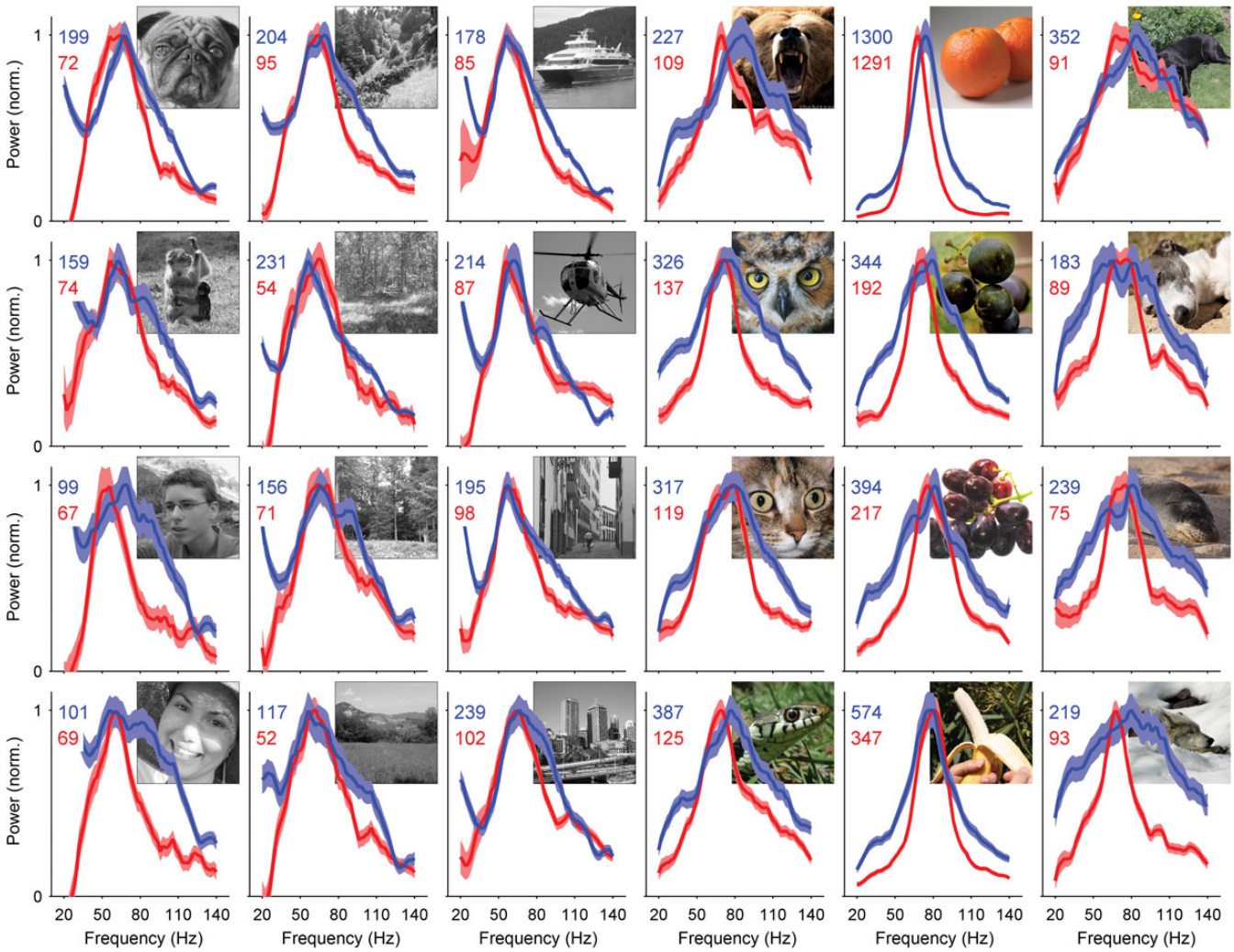

Figure 3. Power change spectra for 12 example grayscale and 12 color images. Each panel shows the natural image presented to the animal and the corresponding spectra (red: monkey P, blue: monkey A) of power changes in percent, comparing free viewing of the respective image with a prestimulus baseline, averaged over all V1 sites (shaded regions indicate ±1 standard error of the mean, SEM). The spectra were scaled such that the lower end of the *y*-axis corresponds to zero change and the upper end corresponds to the percent change value that is indicated in the upper-left corner of the respective panel.

gamma power enhancements are most likely not due to broadband power enhancements as have been found in other ECoG recordings (Miller et al. 2009).

Figure 5*A* shows, for an example V1 site in monkey P, the power change spectrum averaged over all images. Figure 5*B* shows a very similar gamma-band peak in an example site from area V4. In contrast, 2 example sites in parietal and frontal cortex did not show enhanced gamma-band activity during natural viewing (Fig. 5*C*,*D*). Figure 5*E* shows gamma-band power changes, and Figure 5*F* the corresponding *t*-values [comparing log(power) between natural viewing and baseline] across all sites in the ECoG grid. The topographies reveal enhanced gamma-band power primarily in early-to-intermediate visual cortex covered by the subdural grid, that is, areas V1, V2, V4, and TEO. Notably, outside the visual areas, natural viewing slightly reduced gamma-band power when compared with baseline. Figure 5*G*–L confirms these results in monkey A.

Figure 2*B* had suggested that saccades interrupt ongoing gamma-band oscillations. To investigate this further, Figure 6 shows time–frequency analyses aligned to saccades. In both monkeys and in both areas V1 and V4, the sustained presaccade gamma activity with peak power at frequencies of >50 Hz was, after the saccade, replaced by gamma with peak power at a frequency that slid downwards until a frequency of approximately 30–40 Hz was reached (Fig. 6*A*,*B*,*G*,*H*). This 30- to 40-Hz activity peaked at a postsaccadic latency of 76 ms in V1 and 89 ms in V4 (Table 1, upper part). After this, sustained gamma re-established at the typical frequency band. The postsaccadic 30- to 40-Hz activity co-occurred in time with a peak in the event-related potential (ERP; Fig. 6*C*,*D*,*I*,*J*; Table 1, middle part). The time–frequency analysis of the ERP (Fig. 6*E*,*F*,*K*,*L*; Table 1, lower part) showed that the saccade-aligned ERP accounted for only a small fraction of the 30- to 40-Hz activity.

Discussion

We found strong, sustained, and band-limited gamma-band activity in the visual cortex of 2 macaque monkeys during free viewing of natural images. In area V1, this gamma-band activity was present for all natural images tested. Enhanced gamma-band activity during natural viewing occurred over

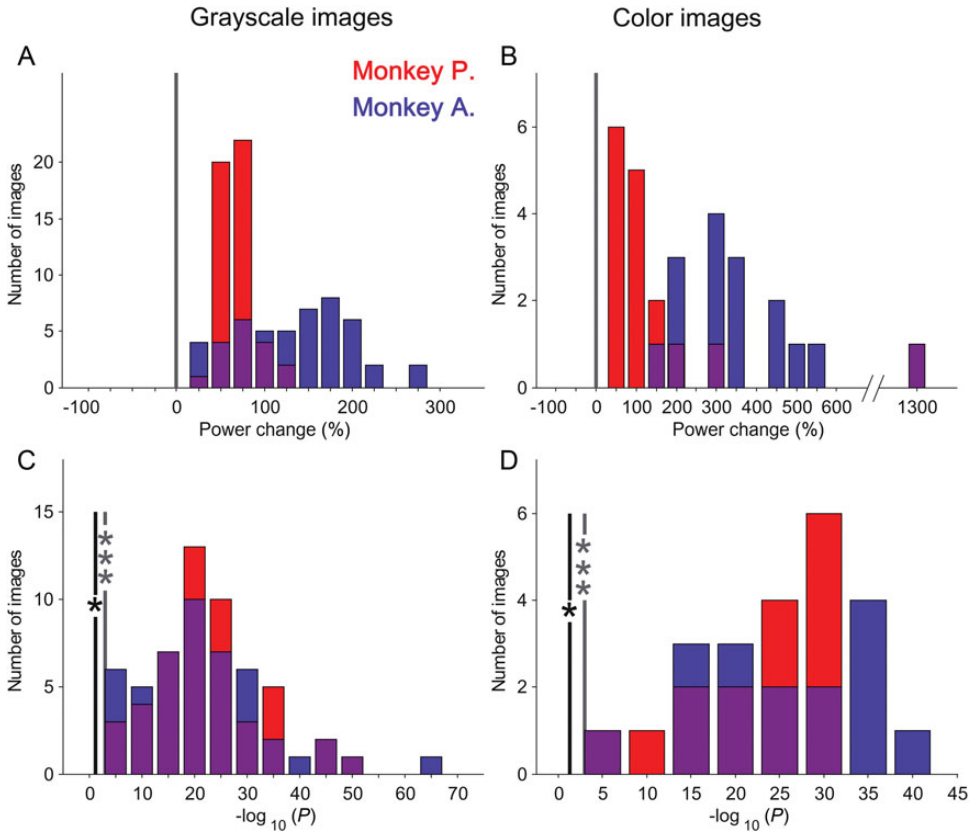

Figure 4. Histograms of gamma power change metrics across all natural images in both monkeys. (*A*) Histograms of changes in peak gamma-band power across all grayscale images, separately for monkey P (red) and monkey A (blue). Purple bar segments correspond to the overlap of histograms of the 2 monkeys. (*B*) Same as (*A*), but for the color images. (*C*) Histograms of the negative decadic logarithm of the *P*-values derived from 2-sided paired *t*-tests comparing gamma-band power (50–80 Hz) between natural viewing and prestimulus fixation baseline, across trials. Color coding as in *A* and *B*. (*D*) Same as in (*C*), but for the color images. Vertical lines indicate significance thresholds of $*P = 0.05$ and $***P = 0.001$.

most of the recorded visual cortex, while it was largely absent over other regions. After saccades, the sustained gamma-band activity of 50–80 Hz was replaced by gamma-band activity with a peak frequency that slid downwards until a frequency of approximately 30–40 Hz was reached at around 80 ms postsaccade. Thereafter gamma-band activity was re-established at the higher frequency.

The strongest gamma-band increases occurred in both monkeys for the orange and the banana photograph. Those fruits were given to the monkeys regularly in their home cage. Thus, the particularly strong gamma-band activity might be due to the familiarity and/or the appetitive character of these stimuli. Future experiments will need to test those predictions directly.

We found gamma-band activity during natural viewing with LFP recordings from an ECoG grid, rather than, for example, with single-unit spike recordings. While this does not allow us to demonstrate gamma-band synchronization in spike trains directly, it is very likely that also the spikes showed gamma-band rhythms. The LFP recordings reflect mainly synaptic currents and the resulting membrane potential fluctuations (Mitzdorf 1985). These synaptic activities, in turn, result from spiking activity, mostly from nearby cortical neurons. Simultaneous recordings of spikes and LFPs have documented that gamma-band power enhancements are typically accompanied by gamma-band, spike-field coherence (Fries, Reynolds, et al. 2001; Fries, Schröder, et al. 2001; Fries et al. 2002, 2008; Pesaran et al. 2002; Womelsdorf et al. 2006; Bosman et al. 2009), suggesting that the spikes are directly related to the population rhythm.

A previous study had investigated visual cortical responses to natural scenes, using recordings from awake cat area 18, while the animals were presented with natural movies (Kayser et al. 2003). These movies induced activity that did not differ significantly from activity induced by visual pink noise, but it did differ strongly from gamma-band activity induced by gratings. We think that the discrepancy to our study is due to their use of a particular type of movies. As stated in that study, "these [movies] were recorded from a camera mounted to a cat's head while the animal was exploring different local environments such as forests and meadows […]." The motion of the cat's head and the mounted camera resulted in strong and frequent movements of the entire image. It has been shown previously that such strong image motion transients lead to stimulus-locked LFP components, which replace the stimulus-induced, gamma-band response (Kruse and Eckhorn 1996). Kruse and Eckhorn had also investigated activity in cat primary visual cortex. When they presented smoothly moving stimuli, this induced gamma-band oscillations. In contrast, when they superimposed onto the smooth stimulus movement dynamically changing accelerations, gamma-band oscillations were replaced by stimulus-locked response components. Thus, when visual stimuli are static or moving smoothly, visual cortex generates neuronal synchronization rhythmically in the

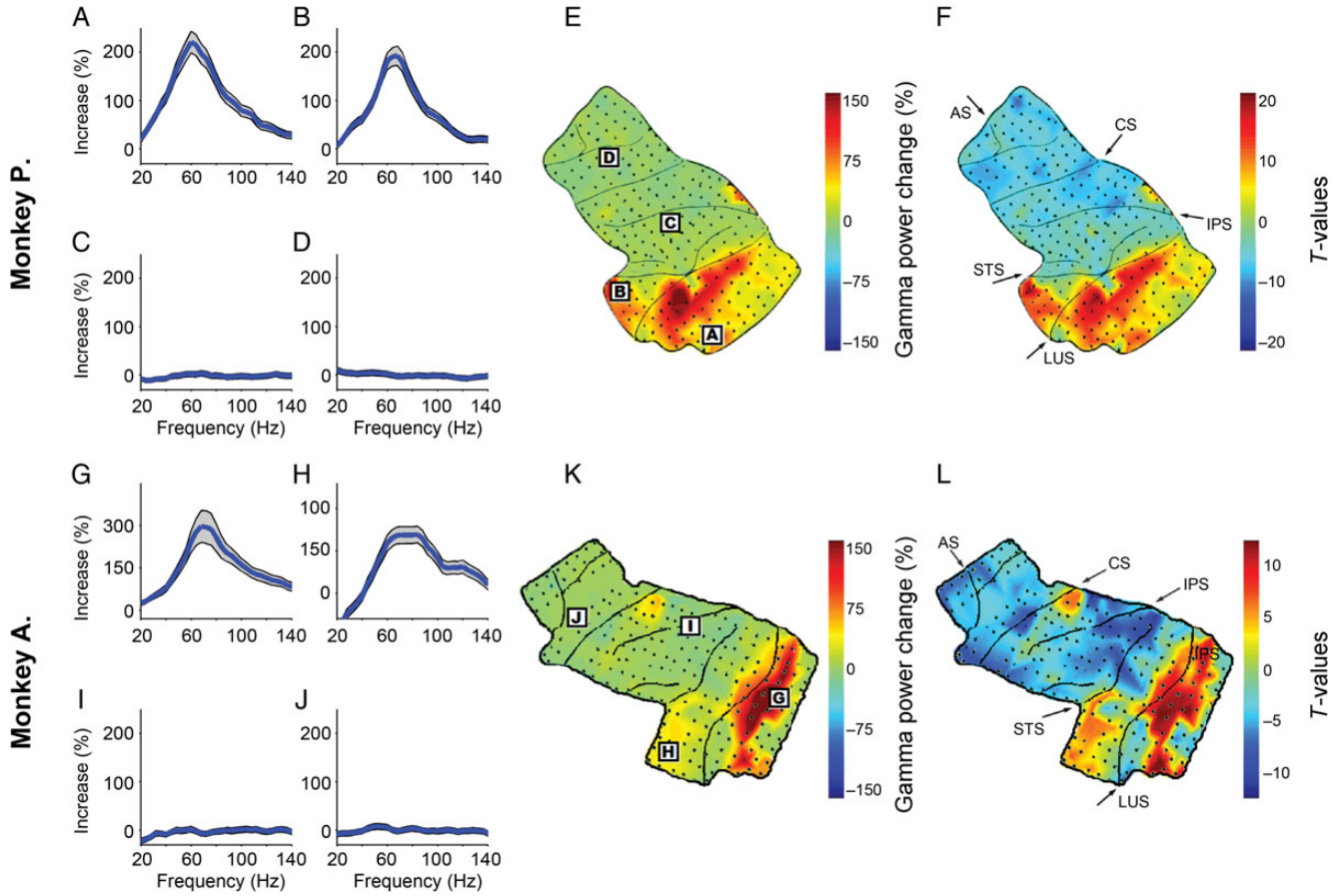

Figure 5. Power change spectra averaged across all natural images for 4 example sites in both monkeys. (*A–D*) Spectra of power change (±1 SEM) during free viewing, when compared with baseline, averaged across all natural images, for the example sites indicated in (*E*). (*E*) Topographical distribution of gamma-band power changes. (*F*) Topographical distribution of the corresponding *t*-values for the comparison of free viewing of natural images versus baseline. (G–*L*) Same analyses as in (*A–F*), but for monkey A. The gamma-band was defined as 50–80 Hz in both monkeys. All analyses shown in this figure use fixation periods in between saccades (see Methods for details). LuS: lunate sulcus; STS: superior temporal sulcus; AS: arcuate sulcus; CS: central sulcus; IPS: intraparietal sulcus.

gamma-frequency band (Friedman-Hill et al. 2000); when the visual input entails unpredictable transients, neurons temporarily synchronize to these stimulus transients (Kruse and Eckhorn 1996). Since synchronization is most likely crucial for the successful communication to postsynaptic targets (Fries 2009), the intrinsically generated neuronal gamma-band synchronization to stimuli without transients is likely subserving their continued signaling, and the externally triggered neuronal synchronization to stimulus transients likely subserves the signaling of salient events in the visually observed world. Typically, such salient events are the appearance or the motion onset of an object within the visual field. Rarely is there a motion transient in our entire visual input due to motion of the entire visual world around us. In contrast, in the movies of Kayser et al., the motion transients regularly affected the entire visual field, as they were generated by movements of the camera mounted on the head of a cat, and they occurred very frequently if not continuously. This condition differs crucially from natural viewing. We note that, during natural viewing, motion transients of the entire visual field do occur, mostly due to saccades. Yet, those transients are generated by the visual system itself and are therefore dealt with in a different way, as is obvious from our perceptual experience. Visual motion transients due to our own eye movements (or body movements) are, in healthy subjects, not experienced as movements of the external world. In contrast, the motion transients in the movies of Kayser et al. are experienced as strong and frequent movements of the entire external world.

Another previous study used actual free viewing of natural images, like in our study, and recorded neuronal activity from area 17 of cebus monkeys (Ito et al. 2011). This study finds that "LFP modulations in the beta frequency range are initiated in V1 with the beginning of saccades," and that "this signal appears to modulate the timing of the onset of visually evoked spiking activity during fixations, leading to a locking of these first spikes to a specific phase of the LFP modulation." The authors compare their finding directly to those of Bosman et al. (2009), particularly with regard to the presence of gamma-band activity in the Bosman et al. study and the lack of it in their study. They suggest that the absence of gamma in their study might be a genuine consequence of the free viewing of natural images, whereas the presence of gamma in the Bosman et al. study might be due to stimulation with high contrast gratings and to fixation with attention to a peripheral target. Our current study shows that, also during free viewing of natural images, strong gamma-band activity is present in early and intermediate visual cortices. It could be argued that one reason for this discrepancy is our use of rhesus monkeys, while Ito et al. used cebus monkeys. However, we think that

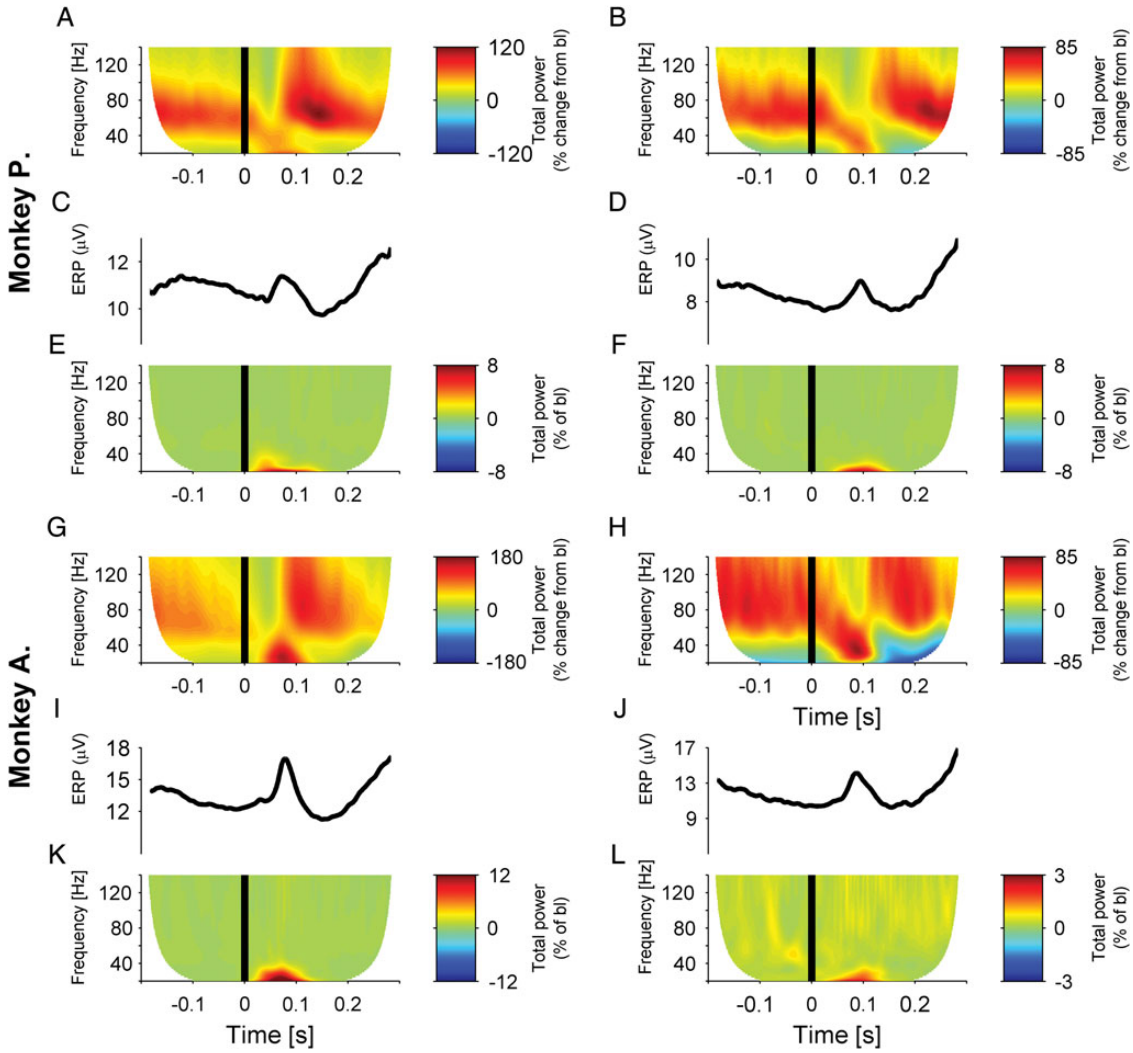

Figure 6. Dynamics of gamma-band power around the time of saccades. (*A*) Time–frequency analysis of power (expressed as percent change from prestimulus baseline) in area V1 around the time of a saccade of monkey P. The saccade is indicated by the vertical black line at time zero (moment of peak saccade velocity). (*B*) Same as (*A*), but for area V4. (*C*) Saccade-aligned ERP (averaged after single-trial rectification) in area V1. (*D*) Same as (*C*), but for area V4. (*E*) Time–frequency analysis of the power of the ERP (expressed as percent of the prestimulus baseline). Note that color scales differ markedly between (*E*) and (*A*). (*F*) Same as (*E*), but for areas V4. (*G–L*) Same as (*A–F*), but for monkey A.

Table 1
Peak latencies of postsaccadic transients

	V1 peak latency (ms)	V4 peak latency (ms)
TFR of LFP		
Monkey P	78	88
Monkey A	74	89
Average	76 ± 3	88.5 ± 1
ERP		
Monkey P	72	95
Monkey A	79	88
Average	75.5 ± 5	91.5 ± 1
TFR of ERP		
Monkey P	70	99
Monkey A	74	88
Average	72 ± 3	93.5 ± 8

The upper part of the table gives the peak latencies of the postsaccadic transient in 30–40 Hz LFP power, separately for V1 and V4, and for the 2 monkeys as well as their mean. The middle part gives the latencies of the postsaccadic peak in the ERP. The bottom part gives the peak latencies of the postsaccadic 30- to 40-Hz power of the ERP.

this species difference is very unlikely to cause the difference, because gamma-band activity has been described across many species, including mouse (Nase et al. 2003) and human (Hoogenboom et al. 2006, 2010), that is, species separated much farther than cebus and rhesus monkeys. Rather, the predominance of beta-band (13–16 Hz) activity in the Ito et al. study might be due to recordings from deep cortical layers. The paper does not specify the laminar origin of the signals, yet another recent study in monkey area V1 demonstrated stimulus-induced 6- to 16-Hz activity to predominate in deep layers (Buffalo et al. 2011), while superficial layers show gamma. The present study used ECoG electrodes placed on the cortical surface. The ECoG signal most likely results from the currents flowing in the tissue under the ECoG electrode. While this signal does not allow to attribute the recorded neuronal currents to particular layers, it is certainly reflecting also the superficial layers, where gamma-band activity is particularly strong (Maier et al. 2010; Buffalo et al. 2011; Xing et al. 2012).

The results described here suggest that gamma-band synchronization is present generally in the visual cortex during natural viewing. This is of great importance for proposals suggesting functional roles for gamma-band synchronization (Singer and Gray 1995; Engel et al. 2001; Fries 2009). Our results suggest that those proposals do not only apply to artificial laboratory conditions, but that they apply also to natural viewing. Future studies will need to test those proposals directly under natural viewing conditions. Combining natural viewing with proper operationalization of the investigated cognitive functions and simultaneously with proper control of basic stimulation conditions will be a challenge.

Funding

This work was supported by grants from the European Science Foundation (European Young Investigator Award to P.F.), the European Union (HEALTH-F2-2008-200728 to P.F.), the LOEWE program ("Neuronale Koordination Forschungsschwerpunkt Frankfurt" to P.F.), the Netherlands organization for scientific research (VICI grant 453-04-002 to P.D.W. and VENI grant 451-09-025 to M.R.), and the Smart Mix Program of the Netherlands Ministry of Economic Affairs and the Netherlands Ministry of Education, Culture, and Science (BrainGain to R.O. and P.F.). Funding to pay the Open Access publication charges for this article was provided by the Ernst Strüngmann Institute (ESI) for Neuroscience in Cooperation with Max Planck Society.

Notes

We thank Edward Chang for help with implanting monkey P, André Grotenhuis for help with implanting monkey A, and Paul Gaalman for help with structural MRI recordings. *Conflict of Interest*: None declared.

References

Bauer M, Oostenveld R, Peeters M, Fries P. 2006. Tactile spatial attention enhances gamma-band activity in somatosensory cortex and reduces low-frequency activity in parieto-occipital areas. J Neurosci. 26:490–501.

Bichot NP, Rossi AF, Desimone R. 2005. Parallel and serial neural mechanisms for visual search in macaque area V4. Science. 308:529–534.

Bosman CA, Schoffelen JM, Brunet N, Oostenveld R, Bastos AM, Womelsdorf T, Rubehn B, Stieglitz T, De Weerd P, Fries P. 2012. Attentional stimulus selection through selective synchronization between monkey visual areas. Neuron. 75:875–888.

Bosman CA, Womelsdorf T, Desimone R, Fries P. 2009. A microsaccadic rhythm modulates gamma-band synchronization and behavior. J Neurosci. 29:9471–9480.

Buffalo EA, Fries P, Landman R, Buschman TJ, Desimone R. 2011. Laminar differences in gamma and alpha coherence in the ventral stream. Proc Natl Acad Sci USA. 108:11262–11267.

Eckhorn R, Bauer R, Jordan W, Brosch M, Kruse W, Munk M, Reitboeck HJ. 1988. Coherent oscillations: a mechanism of feature linking in the visual cortex? Multiple electrode and correlation analyses in the cat. Biol Cybern. 60:121–130.

Engel AK, Fries P, Singer W. 2001. Dynamic predictions: oscillations and synchrony in top-down processing. Nat Rev Neurosci. 2:704–716.

Friedman-Hill S, Maldonado PE, Gray CM. 2000. Dynamics of striate cortical activity in the alert macaque: I. Incidence and stimulus-dependence of gamma-band neuronal oscillations. Cereb Cortex. 10:1105–1116.

Fries P. 2009. Neuronal gamma-band synchronization as a fundamental process in cortical computation. Ann Rev Neurosci. 32:209–224.

Fries P, Reynolds JH, Rorie AE, Desimone R. 2001. Modulation of oscillatory neuronal synchronization by selective visual attention. Science. 291:1560–1563.

Fries P, Roelfsema PR, Engel AK, König P, Singer W. 1997. Synchronization of oscillatory responses in visual cortex correlates with perception in interocular rivalry. Proc Natl Acad Sci USA. 94:12699–12704.

Fries P, Schröder JH, Roelfsema PR, Singer W, Engel AK. 2002. Oscillatory neuronal synchronization in primary visual cortex as a correlate of stimulus selection. J Neurosci. 22:3739–3754.

Fries P, Schröder J, Singer W, Engel AK. 2001. Conditions of perceptual selection and suppression during interocular rivalry in strabismic and normal cats. Vision Res. 41:771–783.

Fries P, Womelsdorf T, Oostenveld R, Desimone R. 2008. The effects of visual stimulation and selective visual attention on rhythmic neuronal synchronization in macaque area V4. J Neurosci. 28:4823–4835.

Gail A, Brinksmeyer HJ, Eckhorn R. 2000. Contour decouples gamma activity across texture representation in monkey striate cortex. Cereb Cortex. 10:840–850.

Gieselmann MA, Thiele A. 2008. Comparison of spatial integration and surround suppression characteristics in spiking activity and the local field potential in macaque V1. Eur J Neurosci. 28:447–459.

Gray CM, König P, Engel AK, Singer W. 1989. Oscillatory responses in cat visual cortex exhibit inter-columnar synchronization which reflects global stimulus properties. Nature. 338:334–337.

Grothe I, Neitzel SD, Mandon S, Kreiter AK. 2012. Switching neuronal inputs by differential modulations of gamma-band phase-coherence. J Neurosci. 32:16172–16180.

Hoogenboom N, Schoffelen JM, Oostenveld R, Fries P. 2010. Visually induced gamma-band activity predicts speed of change detection in humans. NeuroImage. 51:1162–1167.

Hoogenboom N, Schoffelen JM, Oostenveld R, Parkes LM, Fries P. 2006. Localizing human visual gamma-band activity in frequency, time and space. Neuroimage. 29:764–773.

Ito J, Maldonado P, Singer W, Grün S. 2011. Saccade-related modulations of neuronal excitability support synchrony of visually elicited spikes. Cereb Cortex. 21:2482–2497.

Kayser C, Salazar RF, König P. 2003. Responses to natural scenes in cat V1. J Neurophysiology. 90:1910–1920.

Kreiter AK, Singer W. 1996. Stimulus-dependent synchronization of neuronal responses in the visual cortex of the awake macaque monkey. J Neurosci. 16:2381–2396.

Kruse W, Eckhorn R. 1996. Inhibition of sustained gamma oscillations (35–80 Hz) by fast transient responses in cat visual cortex. Proc Natl Acad Sci USA. 93:6112–6117.

Lima B, Singer W, Chen NH, Neuenschwander S. 2010. Synchronization dynamics in response to plaid stimuli in monkey V1. Cereb Cortex. 20:1556–1573.

Livingstone MS. 1996. Oscillatory firing and interneuronal correlations in squirrel monkey striate cortex. J Neurophysiol. 75:2467–2485.

Maier A, Adams GK, Aura C, Leopold DA. 2010. Distinct superficial and deep laminar domains of activity in the visual cortex during rest and stimulation. Front Syst Neurosci. 4:1–11.

Miller KJ, Sorensen LB, Ojemann JG, den Nijs M. 2009. Power-law scaling in the brain surface electric potential. PLoS Comput Biol. 5:e1000609.

Mitra PP, Pesaran B. 1999. Analysis of dynamic brain imaging data. Biophys J. 76:691–708.

Mitzdorf U. 1985. Current source-density method and application in cat cerebral cortex: investigation of evoked potentials and EEG phenomena. Physiol Rev. 65:37–100.

Nase G, Singer W, Monyer H, Engel AK. 2003. Features of neuronal synchrony in mouse visual cortex. J Neurophysiol. 90:1115–1123.

Oostenveld R, Fries P, Maris E, Schoffelen JM. 2011. Fieldtrip: open source software for advanced analysis of MEG, EEG, and invasive electrophysiological data. Comput Intell Neurosci. 2011:156869-.

Pesaran B, Pezaris JS, Sahani M, Mitra PP, Andersen RA. 2002. Temporal structure in neuronal activity during working memory in macaque parietal cortex. Nat Neurosci. 5:805–811.

Ray S, Maunsell JH. 2010. Differences in gamma frequencies across visual cortex restrict their possible use in computation. Neuron. 67:885–896.

Roberts MJ, Lowet E, Brunet NM, Ter Wal M, Tiesinga P, Fries P, De Weerd P. 2013. Robust gamma coherence between macaque V1 and V2 by dynamic frequency matching. Neuron. 78:523–536.

Rubehn B, Bosman C, Oostenveld R, Fries P, Stieglitz T. 2009. A MEMS-based flexible multichannel ECoG-electrode array. J Neural Eng. 6:036003-.

Singer W, Gray CM. 1995. Visual feature integration and the temporal correlation hypothesis. Annu Rev Neurosci. 18:555–586.

Taylor K, Mandon S, Freiwald WA, Kreiter AK. 2005. Coherent oscillatory activity in monkey area v4 predicts successful allocation of attention. Cereb Cortex. 15:1424–1437.

Vinck M, Lima B, Womelsdorf T, Oostenveld R, Singer W, Neuenschwander S, Fries P. 2010. Gamma-phase shifting in awake monkey visual cortex. J Neurosci. 30:1250–1257.

Womelsdorf T, Fries P, Mitra PP, Desimone R. 2006. Gamma-band synchronization in visual cortex predicts speed of change detection. Nature. 439:733–736.

Womelsdorf T, Lima B, Vinck M, Oostenveld R, Singer W, Neuenschwander S, Fries P. 2012. Orientation selectivity and noise correlation in awake monkey area V1 are modulated by the gamma cycle. Proc Natl Acad Sci USA. 109:4302–4307.

Womelsdorf T, Schoffelen JM, Oostenveld R, Singer W, Desimone R, Engel AK, Fries P. 2007. Modulation of neuronal interactions through neuronal synchronization. Science. 316: 1609–1612.

Xing D, Yeh CI, Burns S, Shapley RM. 2012. Laminar analysis of visually evoked activity in the primary visual cortex. Proc Natl Acad Sci USA. 109:13871–13876.